Contrast-enhanced, real-time volumetric ultrasound imaging of tissue perfusion: preliminary results in a rabbit model of testicular torsion

Contrast-enhanced, real-time volumetric ultrasound imaging of tissue perfusion: preliminary results in a rabbit model of testicular torsion

H J Paltiel[1,4]**, H M Padua**[1]**, P C Gargollo**[2,5]**, G M Cannon Jr**[2,6]**, A I Alomari**[1]**, R Yu**[2] **and G T Clement**[3]

[1] Department of Radiology, Children's Hospital Boston and Harvard Medical School, Boston, MA, USA
[2] Department of Urology, Children's Hospital Boston and Harvard Medical School, Boston, MA, USA
[3] Department of Radiology, Brigham and Women's Hospital and Harvard Medical School, Boston, MA, USA

E-mail: harriet.paltiel@childrens.harvard.edu

Abstract

Contrast-enhanced ultrasound (US) imaging is potentially applicable to the clinical investigation of a wide variety of perfusion disorders. Quantitative analysis of perfusion is not widely performed, and is limited by the fact that data are acquired from a single tissue plane, a situation that is unlikely to accurately reflect global perfusion. Real-time perfusion information from a tissue volume in an experimental rabbit model of testicular torsion was obtained with a two-dimensional matrix phased array US transducer. Contrast-enhanced imaging was performed in 20 rabbits during intravenous infusion of the microbubble contrast agent Definity® before and after unilateral testicular torsion and contralateral orchiopexy. The degree of torsion was $0°$ in 4 (sham surgery), $180°$ in 4, $360°$ in 4, $540°$ in 4, and $720°$ in 4. An automated technique was developed to analyze the time history of US image intensity in experimental and control testes. Comparison of mean US intensity rate of change and of ratios between mean US intensity rate of change in experimental and control testes demonstrated good correlation with testicular perfusion and mean perfusion ratios obtained with radiolabeled microspheres, an accepted 'gold standard'. This method is of potential utility in the clinical evaluation of testicular and other organ perfusion.

S Online supplementary data available from stacks.iop.org/PMB/56/2183/mmedia

(Some figures in this article are in colour only in the electronic version)

[4] Author to whom any correspondence should be addressed.
[5] Present address: Department of Urology, Children's Medical Center of Dallas, Dallas, TX, USA.
[6] Present address: Department of Urology, University of Pittsburgh School of Medicine, Pittsburgh, PA, USA.

1. Introduction

Contrast-enhanced ultrasound (US) imaging is potentially applicable to the clinical investigation of a wide variety of perfusion disorders (Eyding *et al* 2002, Abramowicz 2005, Klauser *et al* 2005, Kaufmann *et al* 2007, Lassau *et al* 2007, Lencioni *et al* 2007, Pallwein *et al* 2007, Singh *et al* 2008, Charnley *et al* 2009, Weber 2009). Conventional techniques of contrast-enhanced harmonic US imaging are typically employed in the subjective assessment of organ perfusion. Quantitative analysis of perfusion is not widely performed, and is limited by the fact that data are acquired from a single tissue plane, a situation that is unlikely to accurately reflect global perfusion of the tissue or organ under consideration (Wei *et al* 1998, Wei *et al* 2001, Paltiel *et al* 2006, Thierman *et al* 2006, Su *et al* 2009).

Diagnosis of testicular torsion currently relies on a qualitative determination of reduced testicular perfusion by color Doppler imaging and spectral analysis. Prior investigations have documented limitations of available techniques used to investigate testicular vascular disorders, especially in children, where testicular volumes are relatively small and normal blood flow rates are low (Nussbaum Blask *et al* 2002, Kalfa *et al* 2004, Eaton *et al* 2005, Karmazyn *et al* 2005). In particular, testicular torsion may be difficult to diagnose in the prepubertal population (Choyke 2000). Prompt diagnosis of testicular torsion and surgical intervention are necessary in order to re-establish testicular perfusion as salvage rates are directly related to the duration of ischemia (Koh *et al* 1995). Recent studies by Paltiel *et al* (2006), and Thierman *et al* (2006) have shown that both qualitative and quantitative analyses of perfusion information derived from 2D contrast-enhanced pulse inversion imaging in a rabbit model of testicular ischemia are superior to qualitative analysis of conventional color and power Doppler imaging.

The recent development of matrix-phased array US transducers for three-dimensional (3D) imaging permits real-time interrogation of a tissue volume. To date, these transducers have been largely employed in the investigation of disorders of myocardial contractility and cardiac valvular disease (Pemberton *et al* 2005, Salehian and Chan 2005). However, dynamic imaging of a tissue volume during a constant infusion of contrast material offers a potential method for achieving 4D perfusion information. The goal of our study, therefore, was to exploit the rapid frame rates available with a 2D matrix-phased array US transducer to obtain a real-time, volumetric assessment of testicular parenchymal perfusion in an experimental animal model of unilateral testicular torsion.

2. Materials and methods

2.1. Animal selection

The study was performed according to a protocol approved by the Animal Care and Use Committee of Children's Hospital Boston, in accordance with the Guiding Principles for Research Involving Animals and Human Beings as adopted by The American Physiological Society, and conformed to guidelines issued by the National Institutes of Health for care of laboratory animals. Use of the rabbit in experimental models of testicular ischemia and torsion is well established (Frush *et al* 1995, Coley *et al* 1996, O'Hara *et al* 1996, Brown *et al* 1997, Paltiel *et al* 2006, Thierman *et al* 2006). Twenty adult male New Zealand white rabbits (Millbrook Breeding Labs, Amherst, MA) with a mean weight of 4.4 kg were studied.

2.2. Animal preparation

General anesthesia was induced with glycopyrrolate (American Reagent Laboratories, Inc., Shirley, NY) 0.04 mg kg^{-1} intramuscularly (IM), followed by ketamine (Fort Dodge Animal Health, Overland Park, KS) 10 mg kg^{-1} intravenously (IV), and acepromazine maleate (Fort Dodge Animal Health, Overland Park, KS) 0.5 mg kg^{-1} IV. An endotracheal tube was placed to protect the airway (3-F cuffed tube, Teleflex Medical, Research Triangle Park, NC), and the animals placed on a ventilator. Anesthesia was maintained with 0.25–3% isoflurane (Baxter, Deerfield, IL) mixed with oxygen and delivered via the trachea. A catheter was inserted into an ear vein for purposes of US contrast agent administration (BD Insyte^{TM} Autoguard^{TM}, BD Medical, Sandy, UT). Straight catheters were inserted into the ascending aorta just above the aortic valve (3-F Morpheus$^{®}$ CT PICC, AngioDynamics, Queensbury, NY) for radiolabeled-microsphere injection and into one femoral artery (3-F; Cook, Bloomington, IN) for blood pressure monitoring and for obtaining reference blood samples. Heparin flushes were administered through the venous and arterial catheters. Ambient temperature was held constant. Heart rate, respiratory rate and oxygen saturation were continuously monitored. For pain control prior to scrotal incision and testicular torsion, the rabbits received a bilateral spermatic cord block containing bupivacaine (AstraZeneca, Wilmington, DE) 0.2 mg kg^{-1} and lidocaine (Hospira, Inc., Lake Forest, IL) 1 mg kg^{-1}.

2.3. Surgical procedure

The rabbit fur overlying the scrotum was removed using a commercially available topical depilation agent (Nair^{TM} or Veet$^{®}$).

Following the baseline 3D US studies (see below), bilateral medial, ventral scrotal incisions were made under sterile conditions and the scrotal layers dissected to the tunica vaginalis. The testes were exposed, and unilateral torsion with contralateral orchiopexy was performed. The testes were then secured in place and the overlying scrotum closed. Rabbits underwent either unilateral 0° (sham surgery; $n = 4$), 180° ($n = 4$), 360° ($n = 4$), 540° ($n = 4$) or 720° ($n = 4$) of spermatic cord torsion after which the postoperative 3D US studies were performed. Apart from the sham surgery group where neither testis underwent torsion, each of the remaining experimental groups consisted of two rabbits where the right testis underwent torsion and two rabbits where the left testis underwent torsion. The intra-aortic catheter was always placed via the groin opposite the torsive testis. In the sham surgery group, the intra-aortic inguinal catheter was located in the right groin in three rabbits, and in the left groin in one rabbit.

2.4. Contrast agent administration

The US contrast agent Definity$^{®}$ (Lantheus Medical Imaging, Inc., Billerica, MA) was used in the study. This contrast agent consists of a perflutren lipid-coated microsphere composed of octafluoropropane encapsulated in an outer lipid shell. The mean diameter of the microspheres ranges from 1.1 to 3.3 μm. 1 mL of contrast agent suspension contains a maximum of 1.2×10^{10} perflutren microspheres. 1.3 mL of contrast agent suspension was reconstituted with normal saline (0.9% NaCl solution) to yield a 20 mL solution. The contrast agent solution was placed in a plastic syringe that was connected to the ear vein catheter by means of an infusion pump (model 55–1111; Harvard Apparatus, South Natick, MA). Contrast was infused at a rate of 160 mL h^{-1} for 2 min for both baseline and postoperative studies, resulting in a dose of approximately 0.35 mL of Definity$^{®}$ per study, and a total dose of 0.7 mL of Definity$^{®}$ per experimental animal. Between

Figure 1. The 3D US transducer (black arrow) rests on a gel standoff pad that overlies the rabbit scrotum and is held in place by a mechanical arm.

infusions, the syringe was gently rotated and inverted to re-suspend the contrast agent, which had a tendency to settle out of solution over time.

2.5. Image acquisition

Due to the current impossibility of performing microbubble destruction and reperfusion imaging simultaneously within a tissue volume with a 2D matrix-phased array US transducer, we decided to investigate tissue perfusion during the contrast wash-in phase. Preliminary testing was performed to determine whether such changes were even detectable without harmonic imaging and without first destroying the US microbubbles. These qualitative observations and subsequent analysis of the data from these tests indicated that intensity rise as a function of time could consistently be detected by numeric analysis, even in cases where intensity change was not visually apparent on the US machine display.

3D contrast-enhanced US imaging was performed using an IU22 unit (Philips Medical Systems, Bothell, WA) and a 7–2 MHz matrix-phased array transducer during the continuous IV infusion of Definity® at baseline and immediately postoperatively, as described above. Imaging was performed with the US probe fixed by means of a custom-built mechanical arm over the mid-transverse scrotum so as to include both testes within the field of view. The mechanical arm rested on a non-absorbing, agar-based standoff pad designed specifically for the study in order to provide coupling and to increase the distance between the probe and the testes (figure 1). Conventional gray-scale imaging was performed with the persistence turned off. The dynamic range was set automatically at +50 dB for every study and was not altered following contrast administration.

At baseline and immediately postoperatively, an IV infusion of Definity® was established, delivering a constant infusion of contrast material over the entire imaging period. Volumetric data were acquired uniformly at 1 s sampling intervals over a 2 min period during wash-in

of contrast. We investigated the wash-in phase of contrast tissue enhancement since this approach was expected to yield meaningful data with respect to perfusion differences induced by varying degrees of obstruction of testicular arterial inflow and venous outflow. Unlike standard contrast infusion techniques that use pulse inversion imaging to maximize signal scattering from contrast material, the 3D mode did not have this capability. Furthermore, there was no possibility of delivering a burst of high-energy US pulses into the testicular tissue with the 2D matrix phased-array probe to cause microbubble destruction. Given these limitations, we chose the time image acquisition to be simultaneous with contrast infusion. The resulting 4D dataset represented US spatial and temporal signal intensity, which was log-compressed by the Philips US system software using a standard frequency compounding method to decrease the dynamic range of the intensity data to fit 8 bit, 0–255 pixel values and to decrease speckle noise. All data were subsequently transferred to a personal computer for image processing and analysis.

2.6. Regional perfusion measurements

Reference testicular perfusion measurements were obtained using a radiolabeled microsphere technique (Heymann *et al* 1977, Matsumoto *et al* 1982). Immediately following US evaluation, radiolabeled microspheres were injected into the proximal ascending aorta and a reference arterial blood sample was obtained for subsequent determination of true testicular perfusion. A different radioisotope was used for the baseline (Ruthenium-103) and postoperative (Scandium-46) imaging sessions (PerkinElmer Life and Analytical Sciences, Billerica, MA). Each radioisotope has a unique photon energy and can therefore be measured independently. For every perfusion measurement, a 0.2 mL solution containing 10 μCi (0.74 MBq) of 15 μm diameter radiolabeled microspheres was injected into the ascending aortic catheter and flushed with approximately 5 mL of saline solution over a period of about 20 s. A reference blood sample was simultaneously removed from the femoral artery with a 5 mL syringe and withdrawal pump (model 55-1143; Harvard Apparatus, Holliston, MA) at a rate of 2.0 mL min^{-1} for 1.5 min. The withdrawal interval was measured with an electronic timer. At the conclusion of the experiment, each rabbit was sacrificed with an IV dose of pentobarbital (1 mL/4.5 kg). The testes were then removed and immediately sectioned for regional perfusion determination.

Each testis was used in its entirety for perfusion measurement by sectioning it longitudinally into four strips. The tissue and reference blood samples were weighed on a balance (model AB204; Mettler-Toledo, Greifensee, Switzerland). Radioactivity of the tissue and of the reference blood samples was measured in a deep-well gamma counter (Packard, Downers Grove, IL). Perfusion at each time point was determined by comparing counts for the appropriate radioisotope in the testicular tissue samples with counts in the reference blood samples. Regional perfusion measurements (expressed as (mL g^{-1}) min^{-1} of testicular tissue) for each tissue sample were determined. The perfusion measurements for the four individual tissue strips were averaged to obtain a mean baseline and postoperative perfusion measurement for each testis.

2.7. Image processing

For numeric analysis, the DICOM files were imported into MATLAB$^{®}$ for processing. Images were converted from a raw 4D DICOM format into a 256 (width) $\times$ 176 (height) $\times$ 208 (depth) $\times$ 120 (time) 4D matrix representing the three spatial dimensions and time. Width and height refer to the dimensions parallel to the transducer face. The 7–2 MHz matrix-phased array

transducer has a spatial resolution ranging from 0.22 to 0.27 mm axially × 0.27 to 0.34 mm radially, depending upon the imaging field of view, which was set at maximum for all studies. The temporal resolution was 1 frame s^{-1}.

Since data were acquired from the start of contrast infusion, the time history contained a reference period of several seconds prior to contrast arrival in the testicular tissues. The initial time volume was used as a background reference with all subsequent images subtracted by this reference. Because the pertinent information involved the net change in signal intensity as a function of time, and testicular motion was negligible from frame to frame in the cineloop, subtraction permitted small changes in the data to be more readily detected. Stepping through time, the algorithm calculated mean intensity over volumes containing the right and left testes, respectively. The volume was then divided in half in order to isolate the response from each testis. Justification of this simple method was based on the anatomical separation between the right and left testes, which is located at approximately the midline of each image.

The entire segmented testicular volume was selected as the region-of-interest (ROI) for the right or left testis, respectively. This approach to the selection of the ROI accomplished the goals of automating image processing by removing the subjective element inherent in an arbitrary selection of a smaller ROI (or multiple ROIs) within each testis. In addition, by assessing each testis in its entirety, we increased the chances of detecting focal zones of decreased perfusion.

2.8. Quantitative image analysis

Acquisition of volumetric data and the use of a constant IV infusion of US contrast in place of the more commonly employed bubble disruption in a single plane followed by replenishment merited an examination of the expected wash-in curve behavior. In the case of planar disruption, replenishment has been modeled in the form of a vascular network with blood flowing at varying velocities (Hudson *et al* 2009). This configuration predicts a rapid flow period that saturates to a constant value after approximately 10–20 s. In the case of constant perfusion, a velocity distribution would also be expected, but with the additional complexity of a net increase in bubble density as a function of time due to the constant infusion. This increase would be expected to continue until the bubble outflow is in equilibrium with bubble inflow. This process has been observed to cause an approximately linear rise in contrast echo intensity over a period of about 2–3 min. A nonlinear signal would be expected in the first few seconds, due to a combination of the initial introduction of contrast into the imaging volume and the temporal density increase. However, as contrast fills the volume of interest, this curve would become approximately linear, with a slope proportional to blood flow. Under the assumption that the mass of tissue within the imaging volume is constant, it follows that the curve would likewise be proportional to the perfusion rate.

A linear least squares technique (Björck 1996) was implemented to fit the initial rise-phase of the mean signal intensity for the right and left testicular volumes. Perfusion–fill curves are known to follow a cumulative distribution function (Foss 1970), so this linear fit was understood to represent a first-order Taylor approximation of the curve. The slope of the fit was then determined for each experiment, in order to correlate these values with the radiolabeled microsphere perfusion data. Image intensity was not calibrated to acoustic intensity and therefore recorded in terms of arbitrary units (au), such that the slope was calculated in au per second (au s^{-1}). The standard deviation of the residuals was used to assess error in the fit. In this process, the uncertainty in the curve was determined by calculating the maximum and minimum slopes that fit within 1 standard deviation from the curve using only vertical offsets.

(a) (b)
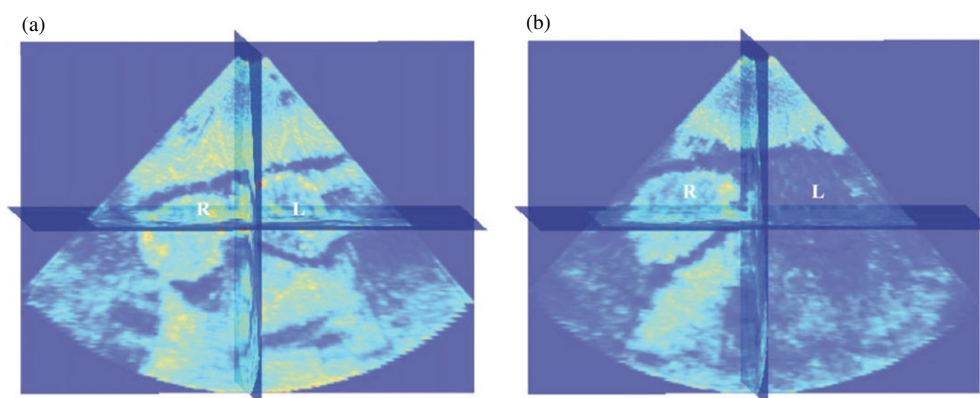
Figure 2. At baseline, the cumulative change in signal intensity for both right (R) and left (L) testes depicted in movie clip 1a available at stacks.iop.org/PMB/56/2183/mmedia is comparable (a). After 720° of left-sided torsion there is a visually obvious decrease in cumulative signal intensity within the left testis compared to the right testis, depicted in movie clip 1b available at stacks.iop.org/PMB/56/2183/mmedia (b).

Both the 3D contrast-enhanced US image intensity data and the radiolabeled microsphere perfusion data were further analyzed by subtracting the baseline values of each experiment from the post-operative values to assess change in the signal intensity rate-of-change relative to the baseline measurement (for US) and change in perfusion (for radiolabeled microspheres).

Since the 3D contrast-enhanced US image intensity data and the radiolabeled microsphere perfusion data are recorded in inherently different units of measurement, in addition to direct calculation of the image intensity slope described above, ratios comparing the mean testicular US signal intensity changes in the intervention (I) testis compared to the contralateral control (C) testis were also determined for both the baseline and postoperative studies. Uncertainty in the ratios was calculated by determining the standard deviation of the data. These ratios were then compared to the I/C testicular perfusion ratios obtained with radiolabeled microspheres.

Scatter plots were used to assess the linear correlation between all baseline and postoperative I/C testicular image intensity ratios obtained with 3D contrast-enhanced US and the perfusion ratios obtained with radiolabeled microspheres. To avoid potential bias caused by the large number of baseline points, all of which are ideally expected to have the same value, a second comparison was also considered, which was restricted solely to postoperative values. Agreement between the postoperative I/C ratios of both techniques was then further examined by plotting the results of each as a function of the degree of torsion.

3. Results

Data from 40 separate experiments were processed by the automated program. Representative imaging data from a mid-scrotal plane within a 3D volume is depicted in the supplementary data available at stacks.iop.org/PMB/56/2183/mmedia.

Processed images (figure 2) reflect the cumulative change in signal intensity:

$$\sum_n \frac{|I_{n+1} - I_n|}{\Delta t}. \tag{1}$$

The graphical output of the MATLAB® program for a series of sample experiments depicting increasing degrees of unilateral testicular torsion is illustrated in figure 3.
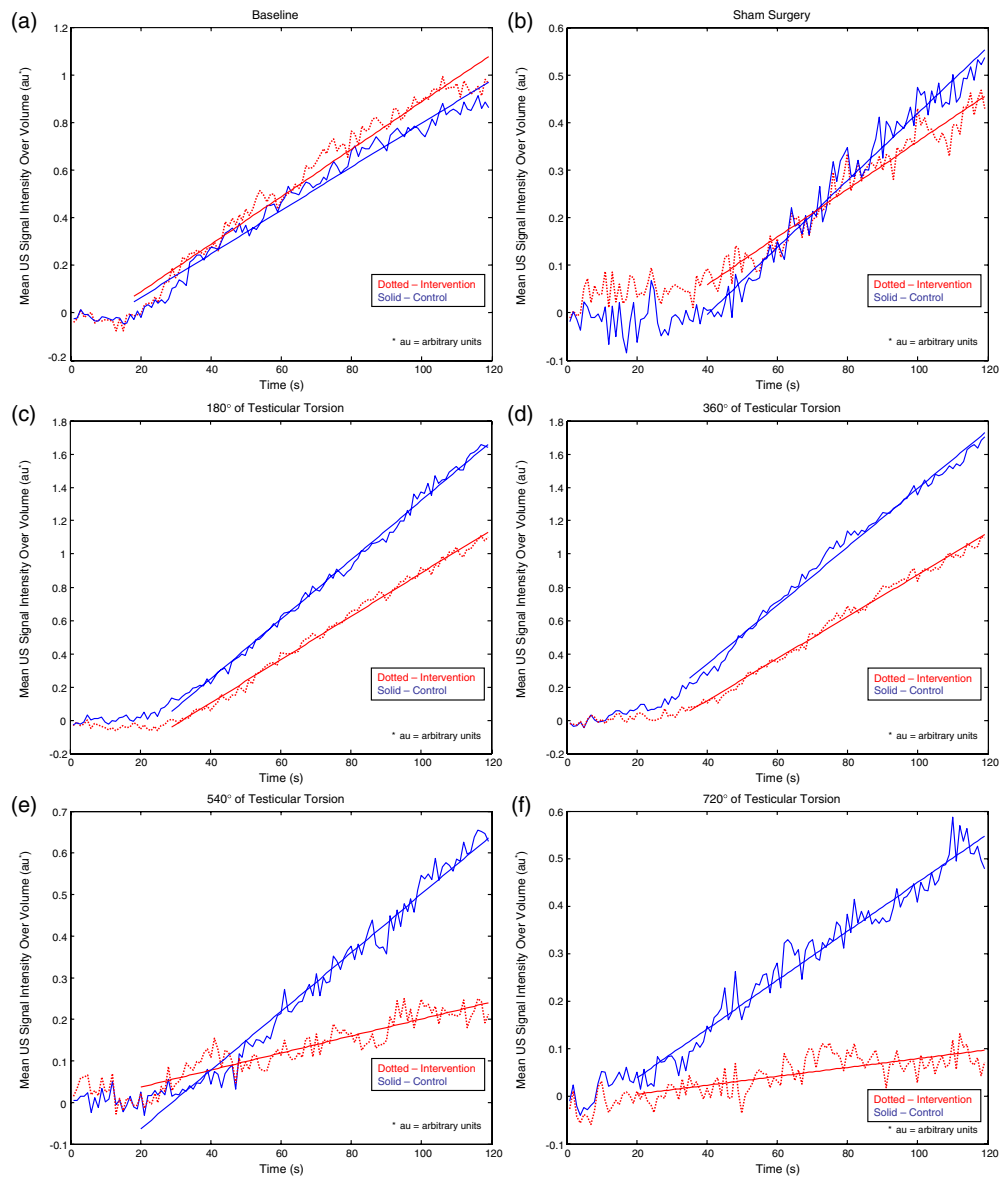
Figure 3. Mean US signal intensity over testicular volume is plotted against time in seconds at baseline (a), after unilateral sham surgery (b), and unilateral torsion of 180° (c), 360° (d), 540° (e) and 720° (f).

Baseline perfusion as measured by radiolabeled microspheres averaged 0.269 mL g^{-1} min^{-1} $\pm$ standard deviation (SD) 0.096 in the intervention testis and 0.269 mL g^{-1} min^{-1} $\pm$ SD 0.093 in the control testis. The baseline radiolabeled microsphere I/C testicular perfusion ratio ranged from 0.71 to 1.48 with a mean of 1.02 $\pm$ SD 0.191. These values were similar whether the intervention side was right or left. The corresponding baseline measurement of the US rate of intensity change (slope) averaged

Table 1. Mean postoperative radiolabeled microsphere-based perfusion measurements and intervention/control testicular perfusion ratios according to the occlusion level.

Occlusion level	No of animals	Perfusion of intervention testis $((mL\ g^{-1})\ min^{-1}) \pm SD$	Perfusion of control testis $((mL\ g^{-1})\ min^{-1}) \pm SD$	Intervention/control testis ratio $\pm$ SD
0° (sham)	4	0.299 ± 0.215	0.315 ± 0.166	0.925 ± 0.342
180°	4	0.254 ± 0.058	0.300 ± 0.060	0.858 ± 0.212
360°	4	0.215 ± 0.065	0.223 ± 0.173	0.972 ± 0.162
540°	4	0.026 ± 0.046	0.275 ± 0.173	0.101 ± 0.185
720°	4	0.003 ± 0.003	0.300 ± 0.091	0.013 ± 0.014

Table 2. Mean postoperative contrast-enhanced 3D ultrasound intensity change and intervention/control testicular intensity ratios according to the occlusion level.

Occlusion level	No of animals	Intensity change intervention testis $(au\ s^{-1}) \pm SD$	Intensity change control testis $(au\ s^{-1}) \pm SD$	Intervention/control testis ratio $\pm$ SD[a]
0° (sham)	4	0.097 ± 0.039	0.107 ± 0.734	1.032 ± 0.286
180°	4	0.139 ± 0.083	0.124 ± 0.069	1.160 ± 0.292
360°	4	0.085 ± 0.092	0.092 ± 0.091	1.300 ± 0.493
540°	4	0.014 ± 0.017	0.081 ± 0.080	0.171 ± 0.221
720°	4	0.023 ± 0.021	0.121 ± 0.112	0.211 ± 0.043

[a] I/C ratios were determined individually for each experiment, followed by calculation of the mean of the ratios for each level of occlusion.

$0.106 \pm SD\ 0.044\ au\ s^{-1}$ in the intervention testis and $0.099 \pm SD\ 0.043\ au\ s^{-1}$ in the control testis. The baseline US slope ratios ranged from 0.70 to 1.84 with a mean of $1.08 \pm SD$ 0.287. These values were similar whether the intervention side was right or left.

After unilateral testicular torsion, perfusion of the intervention testis as measured by radiolabeled microspheres decreased as the degree of occlusion increased, while perfusion of the control testis remained comparatively constant (table 1).

Although the postoperative I/C testicular radiolabeled microsphere perfusion ratio decreased as the severity of testicular torsion increased from milder levels of occlusion (i.e. $\leqslant 360°$) to more severe occlusion (i.e. $\geqslant 540°$, $p < 0.0001$), the perfusion ratios for 0°, 180° and 360° of torsion did not differ significantly ($p \geqslant 0.16$). The corresponding US slope measurements of the intervention testis also generally decreased as a function of occlusion level, although the mildest level of occlusion (180°) was not significantly different from sham surgery (0°), while the US slope measurements of the control testis remained relatively constant. Mirroring the behavior of the postoperative I/C testicular radiolabeled microsphere perfusion ratio, the postoperative contrast-enhanced US I/C testicular signal intensity ratio decreased as the severity of testicular torsion increased from milder levels of occlusion (i.e. $\leqslant 360°$) to more severe levels of occlusion (i.e. $\geqslant 540°$). However, the postoperative US I/C testicular signal intensity ratios for 0°, 180° and 360° of torsion did not differ significantly, ($p \geqslant 0.19$), nor did the ratios for 540° and 720° of torsion (table 2, $p = 0.35$).

Trends in radiolabeled microsphere and 3D contrast-enhanced US imaging measures of testicular parenchymal signal intensity as a function of the degree of torsion are illustrated in figure 4. Inspection of these curves reveals a similar trend between the two measurement techniques.
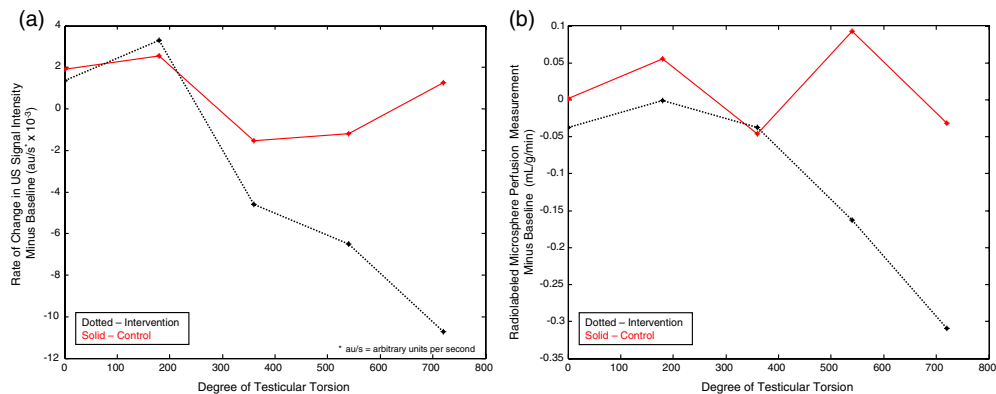
Figure 4. Rate of change in US image intensity as a function of degree of torsion (a) follows a trend resembling that of the radiolabeled microsphere measurements (b). The data for both graphs were plotted after subtracting the baseline from the intervention values for the US and the radiolabeled microsphere measurements, respectively.
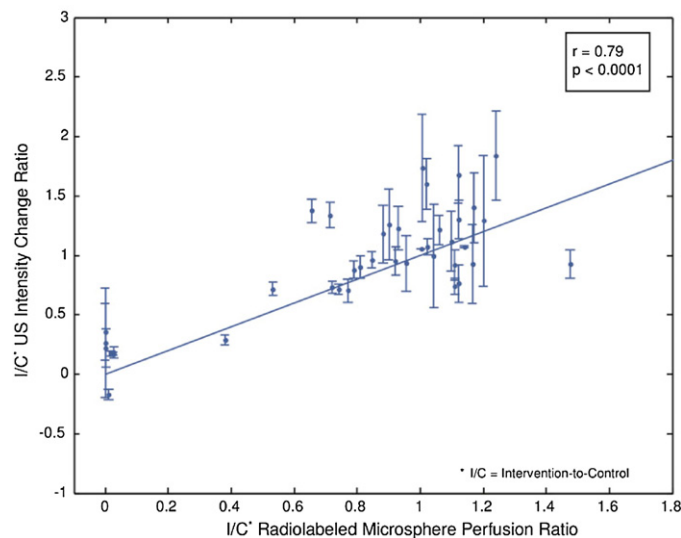
Figure 5. Scatter plot of all baseline and all postoperative 3D contrast-enhanced US I/C intensity rate of change ratios compared to all baseline and postoperative I/C radiolabeled microsphere testicular perfusion ratios.

A scatter plot of all of the 3D contrast-enhanced US I/C testicular signal intensity ratios versus all of the radiolabeled microsphere I/C perfusion ratios (i.e. both baseline and postoperative values) demonstrates a correlation coefficient of 0.79 ($p < 0.0001$, figure 5).

A plot restricted to a comparison of postoperative 3D contrast-enhanced US I/C testicular signal intensity ratios versus the post-operative radiolabeled microsphere I/C testicular perfusion ratios reveals a correlation coefficient of 0.90 ($p < 0.0001$, figure 6).

A scatter plot of all postoperative mean I/C ratios determined by both 3D contrast-enhanced US signal intensity and radiolabeled microsphere testicular perfusion measurements
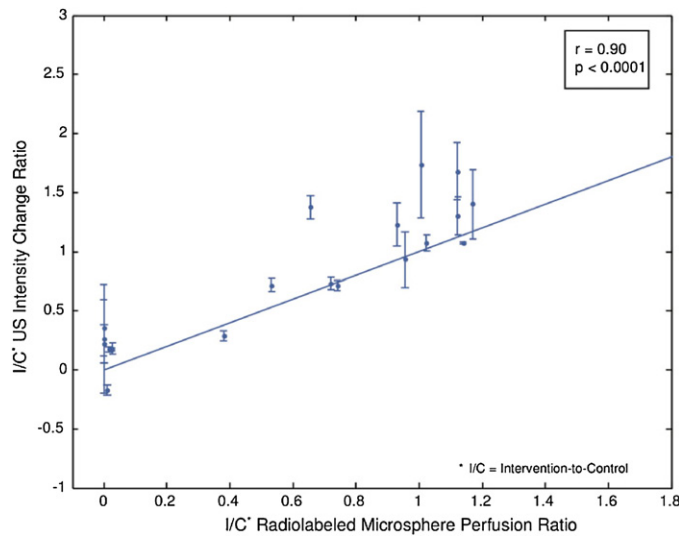
Figure 6. Scatter plot of postoperative 3D contrast-enhanced US I/C intensity rate of change ratios compared to all postoperative I/C radiolabeled microsphere perfusion ratios.
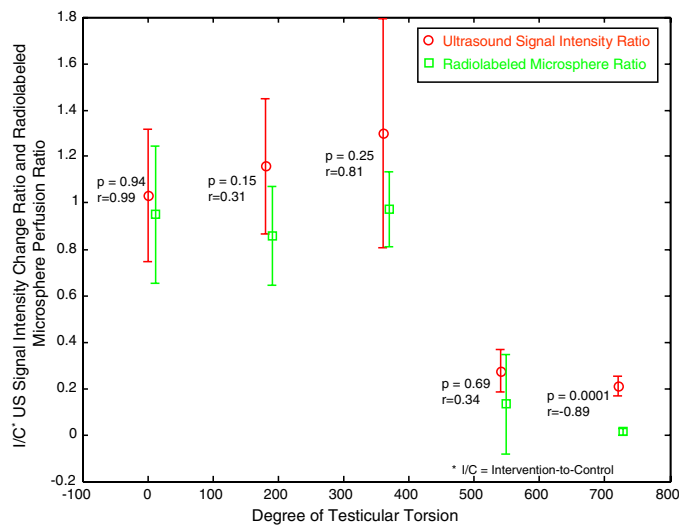
Figure 7. Scatter plot of mean postoperative I/C contrast-enhanced US testicular signal intensity ratios and mean postoperative radiolabeled microsphere testicular perfusion ratios compared to the degree of testicular torsion.

compared to the degree of testicular torsion shows good agreement between the two techniques for all levels of torsion (figure 7).

4. Discussion

In the clinical setting of acute testicular pain, it is critical to accurately determine whether or not the symptomatic testis is ischemic. Large discrepancies in perfusion between

the two testes on conventional US with Doppler evaluation do not usually pose a diagnostic dilemma, whereas more subtle differences may be diagnostically challenging. Clinical US diagnosis of testicular torsion relies on a purely subjective assessment of relative testicular perfusion. Since current clinical examination techniques are not always reliable, the potential contribution of a readily performed, accurate method for analysis of tissue perfusion is considerable.

Contrast-enhanced US imaging of testicular perfusion is an experimental technique not currently approved for clinical use in the United States. In an earlier study by Thierman *et al* (2006), we investigated the use of two automated algorithms in the analysis of perfusion information derived from 2D contrast-enhanced pulse inversion image clips in a rabbit model of testicular ischemia. While these automated methods proved superior to qualitative image analysis by two readers in determining relative testicular perfusion, image analysis was restricted to data acquired from a single tissue plane, which is not necessarily representative of perfusion to the testis as a whole (Paltiel *et al* 2006).

US transducers commonly used in clinical examination of the scrotum do not permit simultaneous acquisition of time-intensity data from multiple tissue planes. However, the 2D matrix-phased array US transducer used in this study did permit the simultaneous acquisition of multiplanar testicular parenchymal signal intensity information. Data from multiple planes yields information about signal intensity change in the direction orthogonal to the image planes, and also provides an opportunity for more accurate alignment between the left and right testes for comparison purposes.

There were several limitations to this investigation: (1) the 2D matrix phased-array transducer used in the study was not designed with volumetric contrast imaging capability in mind. Typical use of US contrast material with conventional 2D imaging involves the initial saturation of the bubbles in the relevant tissue, followed by destruction and rapid reperfusion back to the known initial saturation level. Images are generally acquired using a pulse inversion mode which is not available in 3D. Due to the current impossibility of performing microbubble destruction and reperfusion imaging simultaneously within a tissue volume, investigation of tissue perfusion was restricted to the contrast wash-in phase. Hence, measurement relied on subtle grayscale changes that were often not visible on the unprocessed images; (2) the geometry of the 2D matrix phased-array transducer was not optimal for the performance of scrotal imaging; (3) the size difference between the US contrast agent microbubbles (approximately 15 μm) and the radiolabeled microspheres (approximately 1.1–3.3 μm) is not insubstantial, since vessels of a different order of magnitude are investigated with each technique. Furthermore, the radiolabeled microsphere method of perfusion measurement used as the 'gold' standard in this study is itself subject to error. These facts, in turn, might explain some of the differences in the measurements obtained by the two techniques used in this investigation (Yen and Fung 1978, Bassingthwaighte *et al* 1987, Lindner *et al* 2002); and (4) the automated system used compressed image data that necessarily resulted in limitation of the dynamic range such that the sensitivity to small signal intensity changes may have been compromised.

Neither US contrast nor radiolabeled microspheres permitted an accurate distinction between non-torsion and milder levels of testicular torsion (i.e. < 540°). It has been well documented in the literature that the severity of vascular compromise may vary significantly for a given degree of spermatic cord rotation for reasons that are not entirely clear, although anatomical variability may account for these differences (Bentley *et al* 2004). This variability in ischemic response to testicular torsion is most apparent at lower degrees of testicular torsion, and has been observed in both experimental and clinical settings, in our previous work as well as in the work of others (Frush *et al* 1995, Lee *et al* 1996, Bentley *et al* 2004, Hormann

et al 2004, Paltiel *et al* 2006, Thierman *et al* 2006, Cassar *et al* 2008). Testicular torsion that results in a diminution but not complete cessation of flow to the symptomatic testis is generally referred to as 'partial' or 'incomplete' torsion. The degree of torsion in such cases is usually 360° or less (Lee *et al* 1996, Hormann *et al* 2004). Both techniques employed in this study simply confirmed that testicular perfusion is variably compromised at lower degrees of torsion. As such, the US contrast measurements are an accurate reflection of testicular perfusion.

Although there was a positive correlation between the postoperative I/C contrast-enhanced US testicular signal intensity ratios and mean postoperative radiolabeled microsphere testicular perfusion ratios compared to the degree of testicular torsion when torsion was $\leqslant$ 540°, there was a negative correlation coefficient with a torsion level of 720° (figure 7). We believe that this negative correlation is a result of a systematic offset between the two ratios, i.e. the radiolabeled microsphere ratios trend toward zero, whereas the US contrast ratios never reach zero. A nonzero intensity change measurement might indicate that there is still a small amount of flow into the testis that the microsphere technique cannot detect, or it may simply be a background 'speckle-like' artifact where contrast from outside the volume of interest manifests itself as a positive intensity within the imaging volume.

A potentially fruitful avenue for further investigation may lie in the analysis of change in US microbubble replenishment curve shape induced by varying degrees of testicular torsion. Potdevin *et al* (2004) have shown in phantom experiments that the shape of the replenishment curve is substantially affected by the range of velocities within an ROI. Our preliminary analysis was based on an examination of a simple linear correlation between a 3D contrast-enhanced US microbubble intensity change and a radiolabeled microsphere perfusion measurement. This correlation was performed empirically, without regard to a precise model of anticipated testicular parenchymal perfusion. The US data generally agreed with the 'gold standard' perfusion measurements acquired with radiolabeled microspheres. With both techniques, no significant change was observed between baseline and 180° of torsion, although rates of signal intensity change and radiolabeled microsphere perfusion values decreased with increasing levels of testicular torsion greater than 180°.

For a direct dimensionless comparison of the data, ratios of the I/C testicular measurements with each technique were linearly correlated. Our results suggest that a higher-order fit of the data might result in an even stronger correlation. However, additional data are required to better establish the relevance of this trend. Future work will investigate the underlying equations in order to better predict the relationship between US microbubble signal intensity and testicular parenchymal perfusion.

Of note, in clinical practice, the algorithm used in the current experiment could be implemented in real-time by the US imager, thereby eliminating the need to store and transfer data.

5. Conclusions

Changes in perfusion within a tissue volume can be detected and analyzed with real-time 3D acquisition of US contrast-enhanced images. 3D parenchymal signal intensity measurements are of potential utility in the diagnosis of gonadal torsion, ischemia and infarction of native viscera and organ transplants. Our preliminary data demonstrate good correlation of 3D contrast-enhanced testicular parenchymal US signal intensity measurements with tissue perfusion measurements obtained with radiolabeled microspheres. The results also suggest that a higher-order fit of the US data might result in an even stronger correlation.

Acknowledgments

References

Abramowicz J S 2005 Ultrasonographic contrast media: has the time come in obstetrics and gynecology? *J. Ultrasound Med.* **24** 517–31

Bassingthwaighte J B, Malone M A, Moffett T C, King R B, Little S E, Link J M and Krohn K A 1987 Validity of microsphere depositions for regional myocardial flows *Am. J. Physiol.* **253** H184–93

Bentley D F, Ricchiuti D J, Nasrallah P F and McMahon D R 2004 Spermatic cord torsion with preserved testis perfusion: initial anatomical observations *J. Urol.* **172** 2373–6

Björck Å 1996 *Numerical Methods for Least Squares Problems* (Philadelphia, PA: SIAM)

Brown J M, Taylor K J, Alderman J L, Quedens-Case C and Greener Y 1997 Contrast-enhanced ultrasonographic visualization of gonadal torsion *J. Ultrasound Med.* **16** 309–16

Cassar S, Bhatt S, Paltiel H J and Dogra V S 2008 Role of spectral Doppler sonography in the evaluation of partial testicular torsion *J. Ultrasound Med.* **27** 1629–38

Charnley N, Donaldson S and Price P 2009 Imaging angiogenesis *Methods Mol. Biol.* **467** 25–51

Choyke P L 2000 Dynamic contrast-enhanced MR imaging of the scrotum: reality check *Radiology* **217** 14–5

Coley B D, Frush D P, Babcock D S, O'Hara S M, Lewis A G, Gelfand M J, Bove K E and Sheldon C A 1996 Acute testicular torsion: comparison of unenhanced and contrast-enhanced power Doppler US, color Doppler US, and radionuclide imaging *Radiology* **199** 441–6

Eaton S H, Cendron M A, Estrada C R, Bauer S B, Borer J G, Cilento B G, Diamond D A, Retik A B and Peters C A 2005 Intermittent testicular torsion: diagnostic features and management outcomes *J. Urol.* **174** 1532–5 discussion p 1535

Eyding J, Wilkening W and Postert T 2002 Brain perfusion and ultrasonic imaging techniques *Eur. J. Ultrasound* **16** 91–104

Foss S D 1970 A method of exponential curve fitting by numerical integration *Biometrics* **26** 815–21

Frush D P, Babcock D S, Lewis A G, Paltiel H J, Rupich R, Bove K E and Sheldon C A 1995 Comparison of color Doppler sonography and radionuclide imaging in different degrees of torsion in rabbit testes *Acad. Radiol.* **2** 945–51

Heymann M A, Payne B D, Hoffman J I and Rudolph A M 1977 Blood flow measurements with radionuclide-labeled particles *Prog. Cardiovasc. Dis.* **20** 55–79

Hormann M, Balassy C, Philipp M O and Pumberger W 2004 Imaging of the scrotum in children *Eur. Radiol.* **14** 974–83

Hudson J M, Karshafian R and Burns P N 2009 Quantification of flow using ultrasound and microbubbles: a disruption replenishment model based on physical principles *Ultrasound Med. Biol.* **35** 2007–20

Kalfa N, Veyrac C, Baud C, Couture A, Averous M and Galifer R B 2004 Ultrasonography of the spermatic cord in children with testicular torsion: impact on the surgical strategy *J. Urol.* **172** 1692–5 discussion p 1695

Karmazyn B, Steinberg R, Kornreich L, Freud E, Grozovski S, Schwarz M, Ziv N and Livne P 2005 Clinical and sonographic criteria of acute scrotum in children: a retrospective study of 172 boys *Pediatr. Radiol.* **35** 302–10

Kaufmann B A, Wei K and Lindner J R 2007 Contrast echocardiography *Curr. Probl. Cardiol.* **32** 51–96

Klauser A, Demharter J, De Marchi A, Sureda D, Barile A, Masciocchi C, Faletti C, Schirmer M, Kleffel T and Bohndorf K 2005 Contrast enhanced gray-scale sonography in assessment of joint vascularity in rheumatoid arthritis: results from the IACUS study group *Eur. Radiol.* **15** 2404–10

Koh K B, Dublin N and Light T 1995 Testicular torsion *Aust. N. Z. J. Surg.* **65** 645–6

Lassau N, Chami L, Benatsou B, Peronneau P and Roche A 2007 Dynamic contrast-enhanced ultrasonography (DCE-US) with quantification of tumor perfusion: a new diagnostic tool to evaluate the early effects of antiangiogenic treatment *Eur. Radiol.* **17** (Suppl. 6) F89–98

Lee F T Jr, Winter D B, Madsen F A, Zagzebski J A, Pozniak M A, Chosy S G and Scanlan K A 1996 Conventional color Doppler velocity sonography versus color Doppler energy sonography for the diagnosis of acute experimental torsion of the spermatic cord *AJR. Am. J. Roentgenol.* **167** 785–90

Lencioni R, Della Pina C, Crocetti L, Bozzi E and Cioni D 2007 Clinical management of focal liver lesions: the key role of real-time contrast-enhanced US *Eur. Radiol.* **17** Suppl 6 F73–9

Lindner J R, Song J, Jayaweera A R, Sklenar J and Kaul S 2002 Microvascular rheology of Definity microbubbles after intra-arterial and intravenous administration *J. Am. Soc. Echocardiogr.* **15** 396–403

Matsumoto M, Kimura K, Fujisawa A, Matsuyama T, Asai T, Uyama O, Yoneda S and Abe H 1982 Regional blood flows measured in Mongolian gerbil by a modified microsphere method *Am. J. Physiol.* **242** H990–5

Nussbaum Blask A R, Bulas D, Shalaby-Rana E, Rushton G, Shao C and Majd M 2002 Color Doppler sonography and scintigraphy of the testis: a prospective, comparative analysis in children with acute scrotal pain *Pediatr. Emerg. Care* **18** 67–71

O'Hara S M, Frush D P, Babcock D S, Lewis A G, Barr L L, Bukowski T P, Kline-Fath B M and Sheldon C A 1996 Doppler contrast sonography for detecting reduced perfusion in experimental ischemia of prepubertal rabbit testes *Acad. Radiol.* **3** 319–24

Pallwein L, Mitterberger M, Gradl J, Aigner F, Horninger W, Strasser H, Bartsch G, zur Nedden D and Frauscher F 2007 Value of contrast-enhanced ultrasound and elastography in imaging of prostate cancer *Curr. Opin. Urol.* **17** 39–47

Paltiel H J, Kalish L A, Susaeta R A, Frauscher F, O'Kane P L and Freitas-Filho L G 2006 Pulse-inversion US imaging of testicular ischemia: quantitative and qualitative analyses in a rabbit model *Radiology* **239** 718–29

Pemberton J, Li X, Kenny A, Davies C H, Minette M S and Sahn D J 2005 Real-time 3-dimensional Doppler echocardiography for the assessment of stroke volume: an in vivo human study compared with standard 2-dimensional echocardiography *J. Am. Soc. Echocardiogr.* **18** 1030–6

Potdevin T C, Fowlkes J B, Moskalik A P and Carson P L 2004 Analysis of refill curve shape in ultrasound contrast agent studies *Med. Phys.* **31** 623–32

Salehian O and Chan K L 2005 Impact of three-dimensional echocardiography in valvular heart disease *Curr. Opin. Cardiol.* **20** 122–6

Singh V, Saunders C, Wylie L and Bourke A 2008 New diagnostic techniques for breast cancer detection *Future Oncol.* **4** 501–13

Su H L, Qian Y Q, Wei Z R, He J G, Li G Q, Zhang J, Zhou X D and Jing W 2009 Real-time myocardial contrast echocardiography in rat: infusion versus bolus administration *Ultrasound Med. Biol.* **35** 748–55

Thierman J S, Clement G T, Kalish L A, O'Kane P L, Frauscher F and Paltiel H J 2006 Automated sonographic evaluation of testicular perfusion *Phys. Med. Biol.* **51** 3419–32

Weber M A 2009 Ultrasound in the inflammatory myopathies *Ann. New York Acad. Sci.* **1154** 159–70

Wei K, Jayaweera A R, Firoozan S, Linka A, Skyba D M and Kaul S 1998 Quantification of myocardial blood flow with ultrasound-induced destruction of microbubbles administered as a constant venous infusion *Circulation* **97** 473–83

Wei K, Le E, Bin J P, Coggins M, Thorpe J and Kaul S 2001 Quantification of renal blood flow with contrast-enhanced ultrasound *J. Am. Coll. Cardiol.* **37** 1135–40

Yen R T and Fung Y C 1978 Effect of velocity of distribution on red cell distribution in capillary blood vessels *Am. J. Physiol.* **235** H251–7